

# Chapter 3

## Quantum Dot-Fluorescence-Based Biosensing

**Abstract** Since the emergence of quantum dots (QDs), their excellent fluorescent properties have been widely used in the fabrication of biological sensors for various analytes, such as metal ions, environmental samples, protein, deoxyribonucleic acid (DNA), and ribonucleic acid (RNA). More importantly, some of these sensors can realize not only fixed cell labeling, imaging of live cell dynamics, in situ tissue profiling, but also in vivo animal imaging. A lot of reviews have well summarized these in vitro diagnostic applications and in vivo imaging and sensing applications of QDs. In this chapter, we mainly focus on QDs-fluorescence-based biosensing in DNA, RNA, and DNA microarrays. The introduction of QDs in this aspect promoted the sensitivity, stability, and diversity of DNA and RNA detection obviously.

**Keywords** Quantum dots • DNA biosensor • Fluorescence • RNA analysis • DNA microarray

### 3.1 QDs for DNA Analysis

#### 3.1.1 Main Types for DNA Detection

As illustrated in the introduction part, deoxyribonucleic acid (DNA) biosensing has important significance because of the useful information they possess for disease diagnosis. One simple type of DNA detection systems is based on the hybridization between a DNA target and its complementary probe, where DNA target is commonly directly labeled with QDs. However, such modification of DNA target has less feasibility in practice. For better applications, other types of DNA biosensors such as sandwich structure, competitive system, and molecular beacon (MB) have been studied a lot during the past decades (Fig. 3.1). Fluorescence resonance energy transfer (FRET) has been widely employed in these kinds of DNA biosensors. FRET is a nonradiative process whereby an excited-state donor D (usually a fluorophore) transfers energy to a

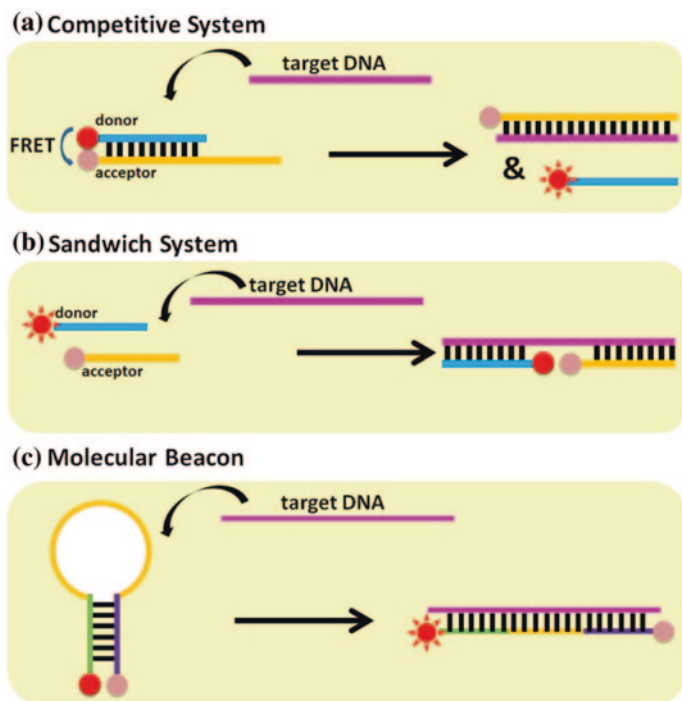


**Fig. 3.1** Main types for DNA detection. **a** competitive system, **b** sandwich system, and **c** molecular beacon structure

proximal ground-state acceptor A through long-range dipole–dipole interactions [1–3]. The acceptor must absorb energy at the emission wavelength(s) of the donor, but does not necessarily have to reemit the energy fluorescently itself. The rate of energy transfer is highly dependent on many factors, such as the extent of spectral overlap, the relative orientation of the transition dipoles, and, most importantly, the distance between the donor and acceptor molecules [4, 5]. FRET is very appealing for bioanalysis because of its simplicity of building ratiometric fluorescent systems. At the beginning, the FRET-based sensing systems were designed with organic dye as donors. With the appearance and development of QDs, more and more QD-based FRET DNA biosensors have emerged. The wide use of QDs as the donors in FRET can be ascribed not only to their high fluorescence quantum yield, strong resistance to photobleaching, but also to their broad excitation wavelengths and narrow and symmetric size-tunable emission spectra. These characteristic properties make their great promise in FRET assays [6]. This method avoided the numerous problems linked to DNA intercalating dyes commonly used for DNA imaging (photobleaching, photoinduced cleavage, and modification of the DNA properties). Krull et al. developed a multiplexed solid-phase nucleic acid hybridization assay on a paper-based platform using multicolor immobilized QDs as donors in FRET, which could reach a detection limit of 90 fmol and an upper limit of dynamic range of 3.5 pmol. As shown in Fig. 3.2, the surface of paper

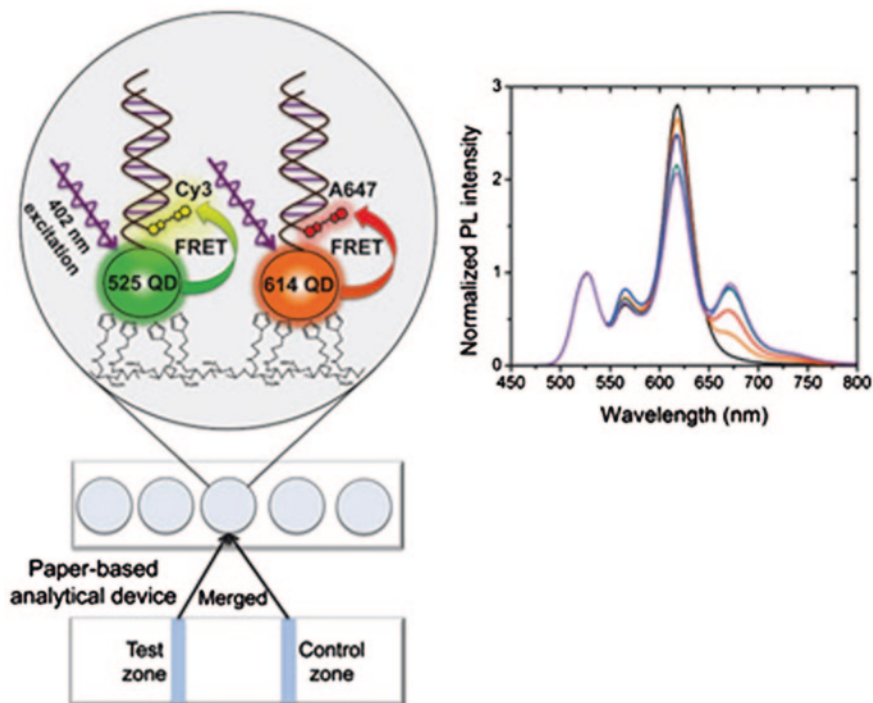


**Fig. 3.2** Design of the paper-based solid-phase multiplexed nucleic acid hybridization assay using multicolor immobilized QDs as donors in FRET. Hybridization with Cy3-labeled SMN1 and A647-labeled target oligonucleotides provided the proximity for FRET-sensitized emission from Cy3 and A647 dyes. Reproduced with permission from Ref. [7]. Copyright 2013, American Chemical Society

was modified with imidazole groups to immobilize two types of QDs–DNA probes. Green-emitting QDs (gQDs) and red-emitting QDs (rQDs) served as donors with Cy3 and Alexa Fluor 647 (A647) as acceptors. The gQD/Cy3 FRET pair served as an internal standard and the rQD/A647 FRET pair served as a detection channel, combining the control and analytical test zones in one physical location. Hybridization of dye-labeled oligonucleotide targets provided the proximity for FRET-sensitized emission from the acceptor dyes, which serves as an analytical signal [7]. Recently, new emerging zero-bandgap carbon nanomaterials, graphene, and graphene oxide (GO) have been widely used as energy acceptors combining with QDs as donors in DNA sensing. He et al. prepared DNA–CdTe by a one-pot method and developed a biosensor based on FRET from the DNA-functionalized CdTe nanocrystals to graphene for the detection of the hepatitis B virus (HBV) surface antigen gene [8].

In a typical sandwich structure, two specific DNA probes are required, i.e., reporter and capture probe. These two probes are labeled with QDs as donor and fluorophore or quencher as acceptor, respectively. They are partly complementary to the target DNA sequence. Thus, in the presence of target DNA, it becomes

sandwiched by reporter and capture probes, which brings the QD donor and fluorophore or quencher acceptor close proximity causing the FRET phenomenon. The detection of decreased fluorescence emission of QDs or increased fluorescence emission intensity of acceptor indicates the presence of target DNA, and their quantification can also be realized. A simple example was demonstrated by Asahi. They developed a sandwich structure for DNA and antigen detection based on self-assembly of multiwalled carbon nanotubes (CNTs) and CdSe quantum dots (QDs) via oligonucleotide hybridization. QDs and CNTs were conjugated with different DNA oligos, which were both complementary to the target DNA. In the presence of target complementary oligonucleotides, QDs and CNTs assembled into nanohybrids via DNA hybridization bringing a fluorescence response to the target DNA amount and a 0.2-pM DNA detection limit was achieved [9]. Huang et al. described a nucleic acid sandwich hybridization assay with a QD-induced FRET reporter system, as shown in Fig. 3.3. Hemagglutinin H5 sequences (60-mer DNA and 630-nt cDNA fragment) of avian influenza viruses were chosen as the target. Two oligonucleotides (16 mers and 18 mers) that complement to the two separate, but neighboring regions of the target sequence were designed as the capturing and reporter probes, respectively. They were conjugated with QD655 (donor) and Alexa Fluor 660 dye (acceptor) at first. The sandwich hybridization occurred once the existence of target

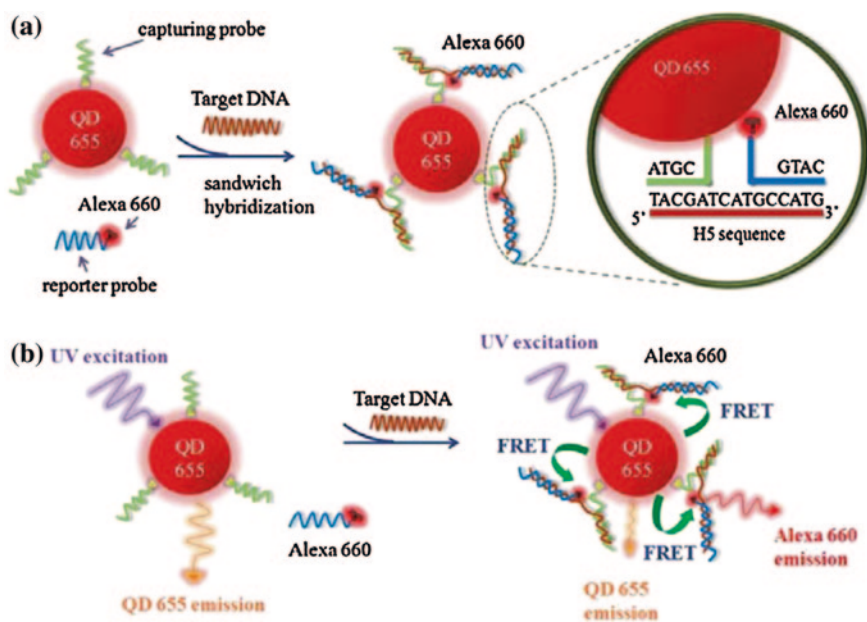


**Fig. 3.3** Schematic illustration of the sandwich hybridization assay with a QD-induced FRET reporter system for H5 target DNA detection. **a** Sandwich hybridization with H5 sequence (target) by the capturing probes conjugated on QD655 (FRET donor) and the reporter probes labeled with Alexa Fluor 660 (FRET acceptor); **b** FRET emission shift before and after the sandwich hybridization. Reproduced with permission from Ref. [10]. Copyright 2012, MDPI AG

sequence causing a FRET signal response, which was monitored by a homemade optical sensor comprising a single 400-nm UV light-emitting diode (LED), optical fibers, and a miniature 16-bit spectrophotometer [10].

In a competitive system, as shown in Fig. 3.1a, two specific DNA probes are required, too. They are labeled with donor and acceptor as the same as those in a sandwich structure. The difference from a sandwich system is that these two DNA probes are complementary to each other and one of them is complementary to the target DNA. In the presence of target DNA, it can compete with probe A to hybridize with probe B to form a more stable duplex. The donor is thus far away from acceptor producing a signal response to the target DNA. Krull demonstrated the use of red-emitting streptavidin-coated QDs (QD(605)) as donors in FRET to introduce a competitive displacement-based assay for the detection of oligonucleotides. QD–DNA bioconjugates featuring 25-mer probe sequences diagnostic of Hsp23 were prepared as capture probe. The hybridization between capture probes and dye-labeled (Alexa Fluor 647) reporter sequences which were partly complementary to capture probe provided a FRET-sensitized emission signal due to proximity of the QD and dye. After competition with target sequence, fully complementary recognition motif embedded within a 98-mer displacer sequence, a nM level for competitive displacement hybridization assays for *in vitro* DNA analysis was achieved [11].

Molecular beacons are oligonucleotide hybridization probes that can report the presence of specific nucleic acids in homogenous solutions. They are hairpin-shaped molecules with a fluorescent label and quencher at each end. QDs are usually employed in MBs as the donor for nucleic acid detection. As shown in Fig. 3.1c, the probe sequence is complementary to target DNA sequence. In the absence of target DNA, a hairpin-like stem-loop structure is formed, causing FRET took place. Once target DNA exists, such hairpin structure is changed into a duplex by the hybridization between probe sequence and target DNA. This causes the separation of QD donor from the quencher, giving a “signal on” response to the target DNA. Mattoussi et al. described the synthesis and characterization of a thiol-reactive hexahistidine peptidic linker that could be chemically attached to thiolated-DNA MB and mediated their self-assembly to CdSe/ZnS core–shell QDs. The hairpin DNA stem structure brought the dye acceptor into close proximity  $r$  of the QD establishing efficient FRET. The presence of DNA complementary to the MB would unwind the stem-loop structure altering the donor–acceptor distance to  $r'$  and changing the FRET efficiency (Fig. 3.4a) [12]. Similarly, Chen et al. described a hybrid fluorescent nanoprobe composed of a nuclease-resistant MB backbone, CdSe/ZnS core–shell QDs as donors, and gold nanoparticles (Au NPs) as quenchers, for the real-time visualization of virus replication in living cells (Fig. 3.4b). A hexahistidine-appended Tat peptide self-assembled onto the QD surface was employed for the noninvasive delivery of the nanoprobe. Upon the existence of the target sequence, coxsackievirus B6 (CVB 6) genome, a 7.3-fold increase in fluorescent signal could be achieved and the real-time detection of infectious viruses as well as the real-time visualization of cell-to-cell virus spreading could be realized [13]. For multiple applications, QDs with different fluorescent emissions have been linked to different MBs, allowing for simultaneous detection within one solution [14]. MBs are extremely target specific, primarily because of the competition

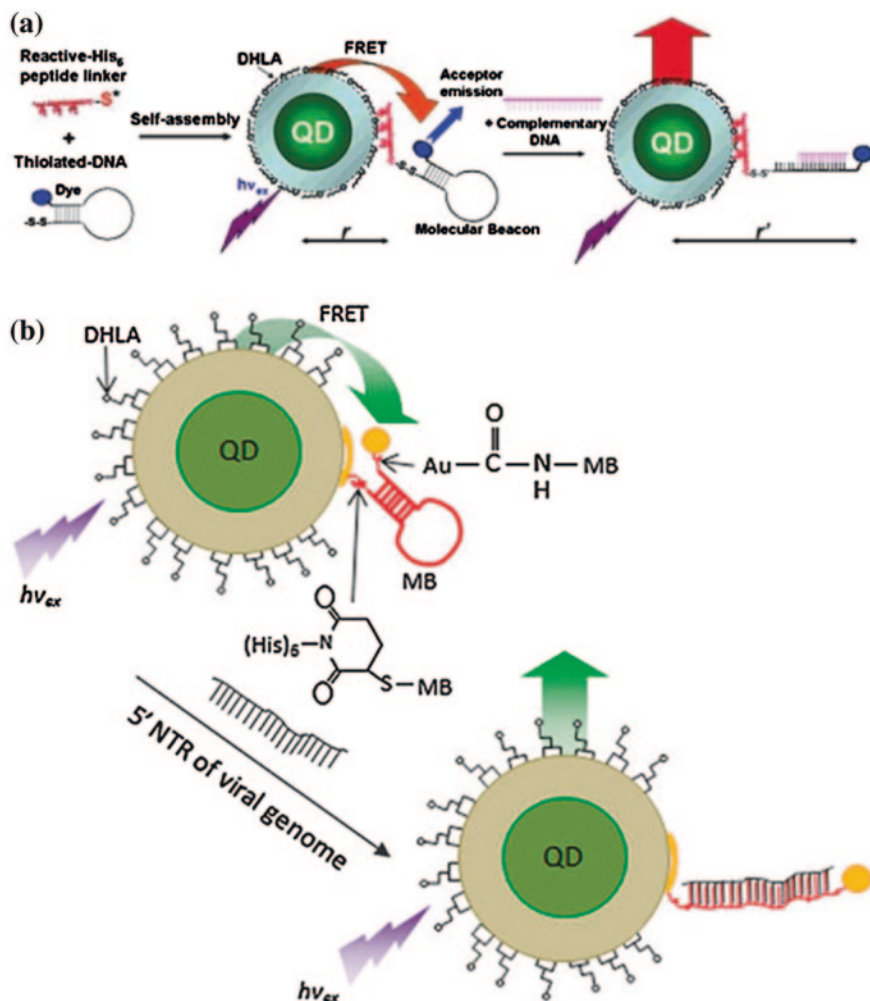


**Fig. 3.4** A schematic representation of His<sub>6</sub>-peptide-linker-facilitated self-assembly of a molecular beacon structure with or without the complementary DNA. Reprinted with the permission from Ref. [12]. Copyright 2007 American Chemical Society (a) and the QD-MB-AuNP probe with or without presence of the complementary viral RNA (b). Reproduced with permission from Ref. [13]. Copyright 2010, Royal Society of Chemistry

between internal hybridization within the stem structure and hybridization between the target and the loop structure [15]. Owing to such high specificity, MB has been commercially used in PCR or reverse transcriptase PCR (RT-PCR) kit. As illustrated above, fluorophore and quencher are tagged to each end of the MB. When the beacon unfolds in the presence of the complementary target sequence, the fluorescence of fluorophore will be recovered. The amount of fluorescence at any given cycle, or following cycling, depends on the amount of specific product and can be easily detected in a thermal cycler. For quantitative PCR, MBs bind to the amplified target following

each cycle of amplification and the resulting signal is proportional to the amount of template. Fluorescence is monitored and reported during each annealing step when the beacon is bound to its complementary target. This information is then used during PCR or RT-PCR experiments to quantify initial copy number. Although lots of QD-based MB systems for DNA, protein, and tumor cell detection have been well documented, no commercial kit has been found in the market yet.

A phenomenon that electron transfer between QDs and DNA induces QD emission quenching is attractive for the development of label-free DNA detection and delivery systems. Clapp et al. designed a pH-responsive pentablock copolymer to form stable complexes with plasmid DNA via tertiary amine segments for potential use in gene delivery monitoring. As shown in Fig. 3.5, QDs can be quenched by the free pentablock copolymer or free DNA, but not by penta/DNA complex. Once polyplex dissociates, the released pentablock copolymer and DNA will lead to QD quenching, and thus, polyplex dissociation can be monitored with the decrease in QD fluorescence. Good behavior of QDs in monitoring the dissociation of pentablock copolymer/DNA polyplexes in vitro was demonstrated in this report, but further application for studying the release of DNA within cells did not realize [16]. Weil et al. prepared a protein-derived biopolymer coating for

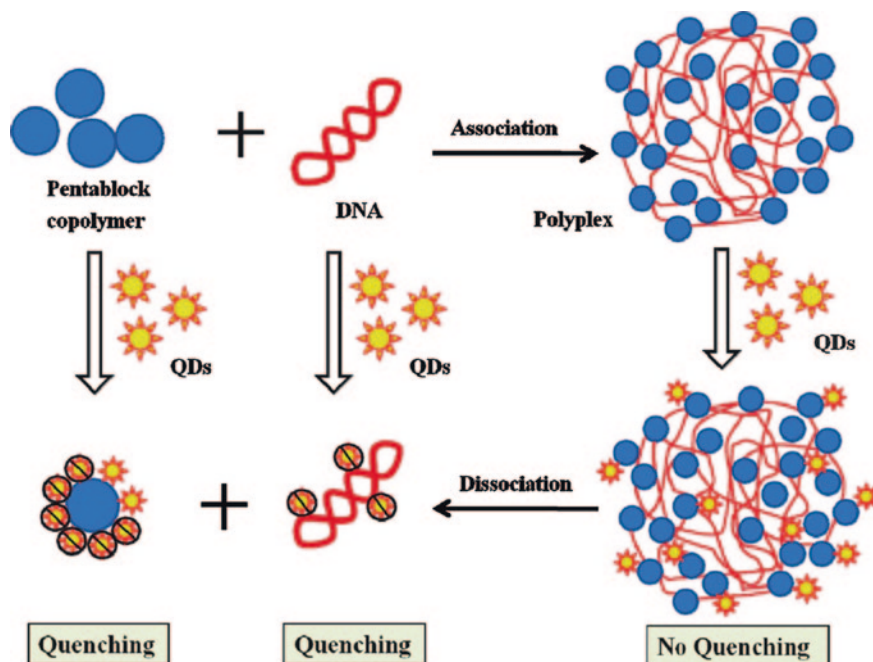


**Fig. 3.5** Schematic illustration of the mechanism of sensing pentablock copolymer/DNA polyplex dissociation using QDs. QDs can be quenched by the free pentablock copolymer and/or free DNA, but not by penta/DNA polyplex. Once polyplex dissociates, the released pentablock copolymer and DNA will lead to QD quenching in such a way that polyplex dissociation can be monitored with the decrease in QD fluorescence. Reproduced with permission from Ref. [16]. Copyright 2011, American Chemical Society

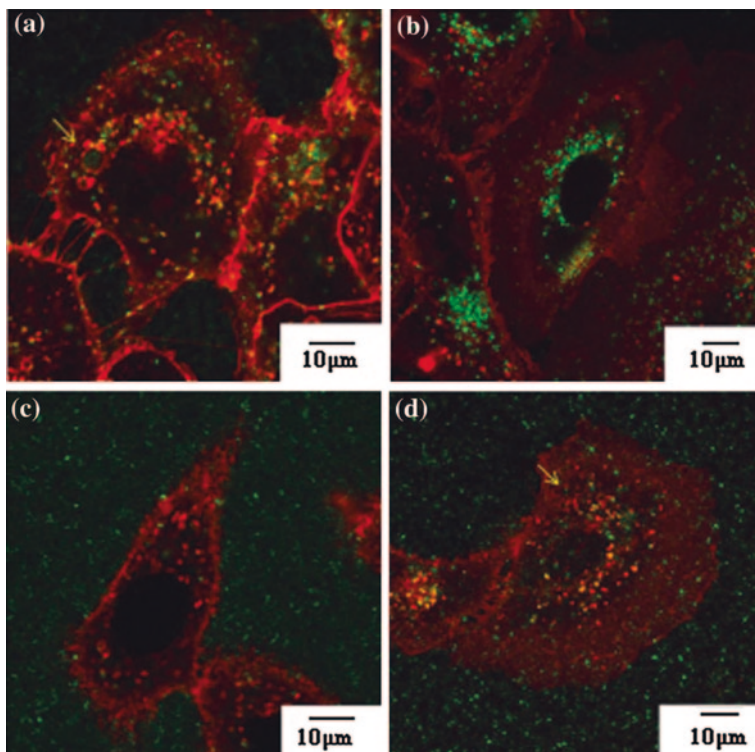


**Fig. 3.6** Confocal imaging of cBSA-QDs and cBSA-QD/DNA complexes. **a** cBSA-QDs incubated with A549 cells for 5 h. **b** cBSA-QDs incubated with A549 cells for 24 h. **c** cBSA-QD/DNA complexed incubated with A549 cells for 5 h. **d** cBSA-QD/DNA complexed incubated with A549 cells for 24 h. Cell membranes were labeled with CellMask Deep Red tracker and are shown in *red color*, and cBSA-QDs are shown as *green points*. Reproduced with permission from Ref. [17]. Copyright 2012, Wiley

efficiently encapsulating QDs which are highly photoresponsive to DNA. Once cBSA-QD/DNA complex were formed, a decrease in the emission intensity of QDs could be observed with increasing DNA content. They realized the intracellular gene delivery tracking. The quenched fluorescence intensity of cBSA-QD/DNA complexes at the beginning of the gene transfection experiment was recovered after DNA release after 24 h (Fig. 3.6) [17].

### 3.1.2 Multiplex DNA Detection

A powerful advantage of QDs in DNA sensing lies in their ability in multiplex DNA detection, which is ascribed to their size-tunable photoluminescence and the broad absorption spectra with narrow emission bands. Broad absorption spectra allow multiple QDs to be excited with a single light source, simplifying



instrumental design, increasing detection speed, and lowering cost. QD emission bands can be as narrow as 20 nm in the visible range, enabling distinct signals to be detected simultaneously with very little cross talk [18]. In 2001, Nie's group achieved multicolor optical coding for biological assays by embedding different-sized QDs into polymeric microbeads at precisely controlled ratios. They designed a model DNA hybridization system using oligonucleotide probes and triple-color-encoded beads and the coding signals could identify different DNA sequences [19].

In 2005, Zhang et al. developed a sandwich type DNA nanosensor based on single quantum dot. They chose CdSe/ZnS core-shell nanocrystals as donors and Cy5 as acceptors. As shown in Fig. 3.7, reporter probe was labeled with Cy5, and capture probe was modified with biotin to conjugate with streptavidin functionalized QDs. When a target DNA was present in solution, it was sandwiched by the two probes. Several sandwiched hybrids were then captured by a single QD through biotin-streptavidin binding, resulting in a local concentration of targets in a nanoscale domain. The occurrence of FRET enabled the detection of low concentrations of DNA in a separation-free format. The functions of QD are not only as a FRET energy donor but also a target concentrator to amplify the target signal

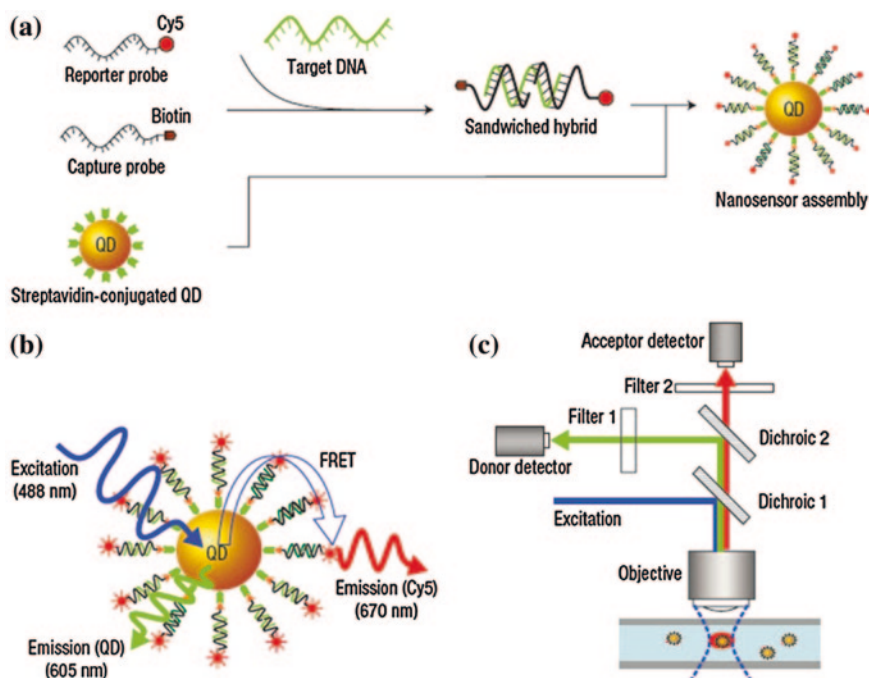


**Fig. 3.7** Schematic of single QD-based DNA nanosensors. **a** Conceptual scheme showing the formation of a nanosensor assembly in the presence of targets. **b** Fluorescence emission from Cy5 on illumination on QD caused by FRET between Cy5 acceptors and a QD donor in a nanosensor assembly. **c** Experimental setup. Reproduced with permission from Ref. [21]. Copyright 2005, Macmillan Publishers Ltd

[20]. The size-tunable photoluminescence and the broad absorption spectra of QDs enable their great promise in multiplex DNA biosensing. In 2010, they successfully applied this similar proposal for multiplex DNA detection [21].

Recently, they further improved their design and described a liposome/QD-based single-particle detection technique for multiple DNA targets with attomolar sensitivity even without the involvement of any amplification step. As shown in Fig. 3.8, the carboxyl-functionalized liposome/QD (L/QD) complex and carboxyl-modified magnetic beads were covalently conjugated with the amino-terminated oligonucleotides, producing the reporter probe and the capture probe, respectively. The presence of target DNA leads to the generation of a sandwich hybrid containing L/QD complexes and results in the release of QDs, which can be sensitively counted by single-particle detection. They designed two sets of probes for the simultaneously determination of HIV-1 and HIV-2 [22].

QD barcodes are another popular approach for multiplexed DNA sensing. Chan et al. used the continuous flow focusing technique to create over 100 different

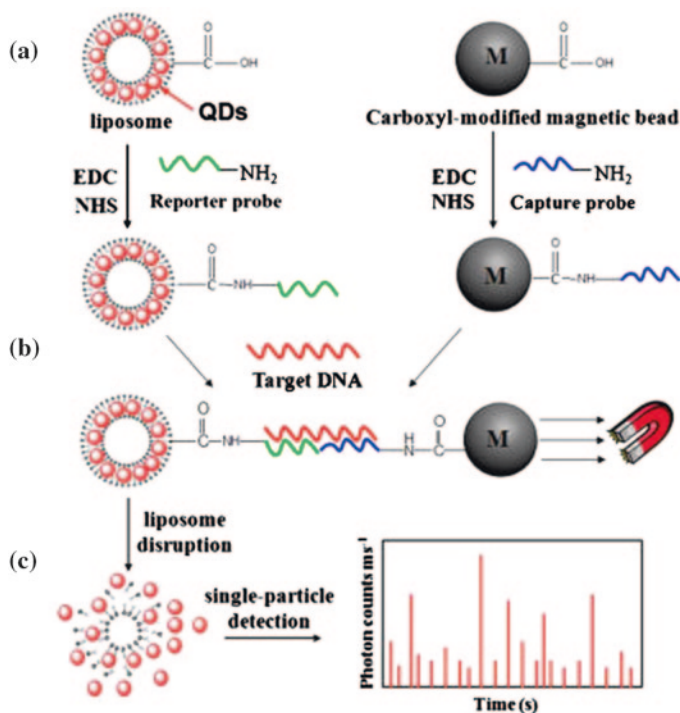


**Fig. 3.8** Design principle of liposome/QD complex-based single-particle detection technique. **a** L/QD complexes, L/QD complex-tagged reporter probes and magnetic bead-modified capture probes were prepared first. **b** Formation of sandwich hybrids in the presence of target DNA and further purification by magnet. **c** Release of QDs from L/QD complex and subsequent measurement by single-particle detection. Reproduced with permission from Ref. [22]. Copyright 2013, American Chemical Society

barcodes using combinations of different emitting QDs. For application, they developed QD barcode-based assay for multiplex analysis of nine different gene fragments from pathogens such as hepatitis B (HBV), SK102 HIV-1, and HCV. Nine barcodes were prepared by mixing a combination of two different emitting QDs (500 and 600 nm) with the polymer poly(styrene-co-maleic anhydride) in chloroform. Different emitting QD barcodes were conjugated with different capture strands, and a secondary oligonucleotide was conjugated with the dye Alexa Fluor 647. A library of QD barcodes conjugated with capture strands are mixed with the secondary oligonucleotide–Alexa Fluor 647 (denoted as SA). When the target sequence was introduced, a sandwich structure of QD barcode-capture strand/target sequence/SA was formed. By measuring the optical emission of this assembled complex in a flow cytometer, a signal response to the target sequence was observed. It showed the great potential of QD in rapid gene mapping and infectious disease detection [23].

## 3.2 QDs for RNA Detection

Ribonucleic acid is a ubiquitous family of large biological molecules that perform multiple vital roles in the coding, decoding, regulation, and expression of genes, including mRNA, tRNA, rRNA, snRNAs, and other noncoding RNAs. Together with DNA, RNA comprises the nucleic acids, which, along with proteins, constitute the three major macromolecules essential for all known forms of life. Like DNA, RNA is assembled as a chain of nucleotides. One of the major differences between DNA and RNA is the sugar, with 2-deoxyribose being replaced by the alternative pentose sugar ribose in RNA. The four bases found in DNA are adenine (abbreviated A), cytosine (C), guanine (G), and thymine (T). A fifth pyrimidine base, called uracil (U), usually takes the place of thymine in RNA and differs from thymine by lacking a methyl group on its ring. Table 3.1 shows the other differences between DNA and RNA.

Some noncoding RNAs such as siRNA, miRNA, and mRNA have attracted more attention because these RNAs play important roles in regulating proteins and associated with various types of human cancers [24–26]. The sensitive and selective detection of RNAs is of great importance in the early clinical diagnosis of cancers, as well as drug discovery. Northern blotting, quantitative, real-time PCR (qRT-PCR), and microarray-based hybridization are the widely used standard methods for analyzing RNAs [27–31]. However, these methods have some limitations such as poor reproducibility with interference from cross-hybridization, low selectivity, insufficient sensitivity, time-consuming, or large amounts of sample required. Thus, the innovative new tools for rapid, specific, and sensitive detection of RNAs are an important field of research. As we know, although some differences exist between DNA and RNA, the chemical structure of RNA is very similar to that of DNA. Therefore, we can detect RNA according to the methods of DNAs. QDs have been successfully conjugated with DNA and used in many applications [32, 33]. The

**Table 3.1** Comparison between DNA and RNA

	DNA	RNA
Stands for	Deoxyribonucleic acid	Ribonucleic acid
Definition	A nucleic acid that contains the genetic instructions used in the development and functioning of all modern living organisms (scientists believe that RNA may have been the main genetic material in primitive life forms)	A single-stranded chain of alternating phosphate and ribose units with the bases adenine, guanine, cytosine, and uracil bonded to the ribose. RNA molecules are involved in protein synthesis and sometimes in the transmission of genetic information
Job/role	Medium of long-term storage and transmission of genetic information	Transfer the genetic code needed for the creation of proteins from the nucleus to the ribosome
Unique features	The helix geometry of DNA is of B-form. DNA is completely protected by the body, i.e., the body destroys enzymes that cleave DNA. DNA can be damaged by exposure to ultraviolet rays	The helix geometry of RNA is of A-form. RNA strands are continually made, broken down, and reused. RNA is more resistant to damage by ultraviolet rays
Predominant structure	Double-stranded molecule with a long chain of nucleotides	A single-stranded molecule in most of its biological roles and has a shorter chain of nucleotides
Bases and sugars	Deoxyribose sugar; phosphate backbone; four bases: adenine, guanine, cytosine, and thymine	Ribose sugar; phosphate backbone. Four bases: adenine, guanine, cytosine, and uracil
Pairing of bases	A–T (adenine–thymine), G–C (guanine–cytosine)	A–U (adenine–uracil), G–C (guanine–cytosine)
Stability	Deoxyribose sugar in DNA is less reactive because of C–H bonds. Stable in alkaline conditions. DNA has smaller grooves, which makes it harder for enzymes to “attack” DNA	Ribose sugar is more reactive because of C–OH (hydroxyl) bonds. Not stable in alkaline conditions. RNA has larger grooves, which makes it easier to be attacked by enzymes
Propagation	DNA is self-replicating	RNA is synthesized from DNA when needed

unique luminescence properties of semiconductor QDs also show a great potential to develop RNA sensors by implementing the QDs as luminescent labels.

### 3.2.1 Direct Fluorescence Labeling

QDs have high extinction coefficient and high quantum yield, which should dramatically increase the sensitivity in theory. Therefore, it was thought that the direct labeling of miRNA with QDs could be well used in miRNA detection and applied in microarray. Liang et al. realized microRNA detection in a microarray configuration

based on the hybridization of target RNA with a capture probe attached to a solid support (shown in Fig. 3.9) [34]. 3'-termini biotinylated miRNA targets hybridized with the corresponding complementary DNA probes, which were immobilized on glass slides. Streptavidin-modified QDs were conjugated with the biotin-miRNA to read out signal (Fig. 3.9a and b). Analysis of a model system indicated that the detection limit for analyzing miRNA was about 0.4 fmol and the detection dynamic range spanned across two orders of magnitude, from 156 to 20,000 pM (Fig. 3.9c). Moreover, the method was applied to develop an assay for profiling 11 miRNA targets from rice (Fig. 3.9d). However, the lack of orthogonal conjugation methods for attaching miRNAs to QDs did not allow the use of different QD colors.

To achieve signal enhancement and multiplexed analysis, QD nanobarcode-based microbead random array platform for accurate and reproducible gene expression profiling in a high-throughput and multiplexed format was developed as shown in Fig. 3.10 [35]. Four different sizes (and thus four different fluorescent colors) of Qdots, with emissions at 525, 545, 565, and 585 nm, are mixed with a polymer

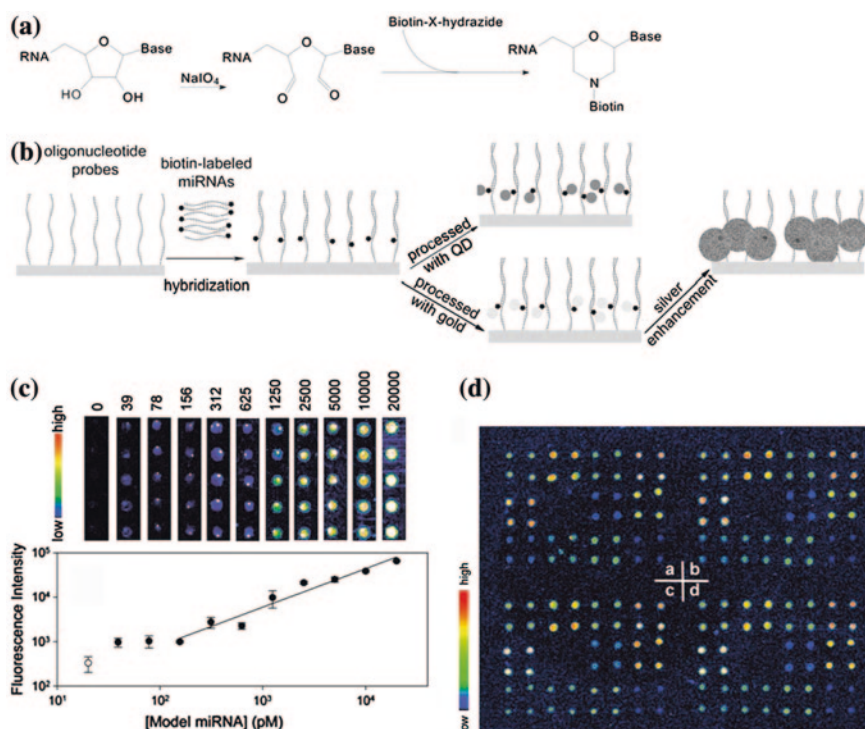


**Fig. 3.9** Analysis of miRNA by means of fluorescent QDs. **a** Principle of labeling miRNA at 3' termini with biotin. **b** Organization of the streptavidin-labeled QDs on a DNA/miRNA duplex bound to a glass support. **c** Fluorescence intensities detected upon analyzing different concentrations of a target miRNA (*upper panel*) and derived calibration curve (*lower panel*). **d** Analysis in an array format of 11 target miRNAs from rice. Reproduced with permission from Ref. [34]. Copyright 2005, Oxford University Press

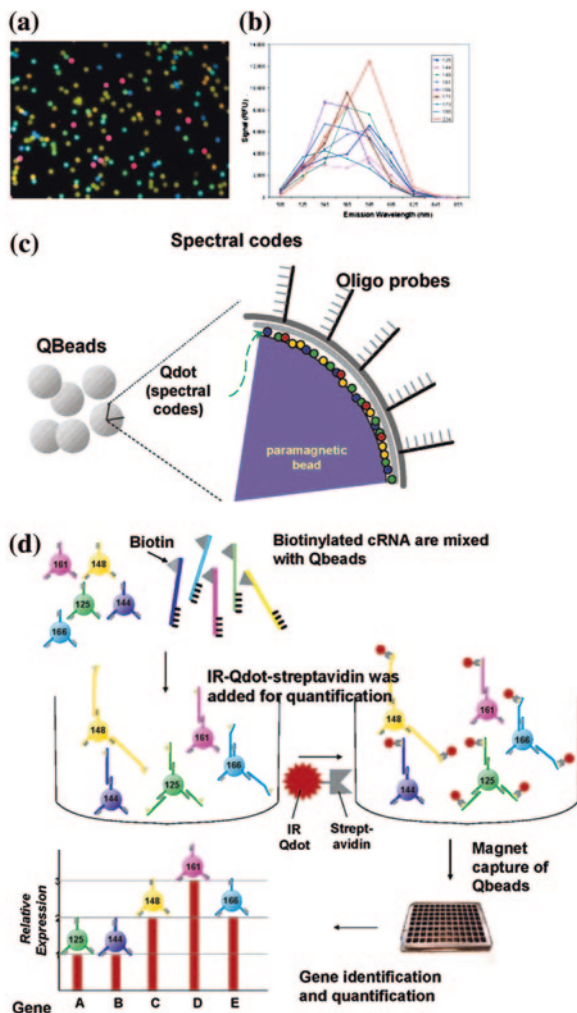


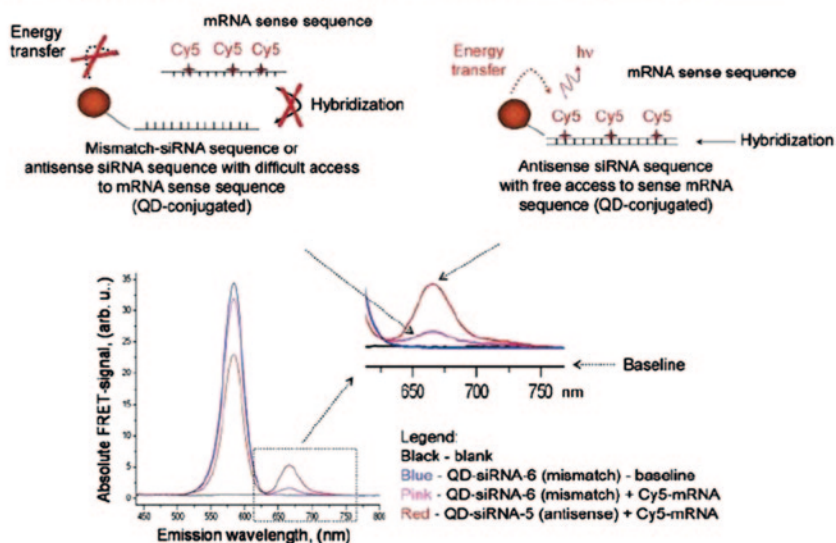
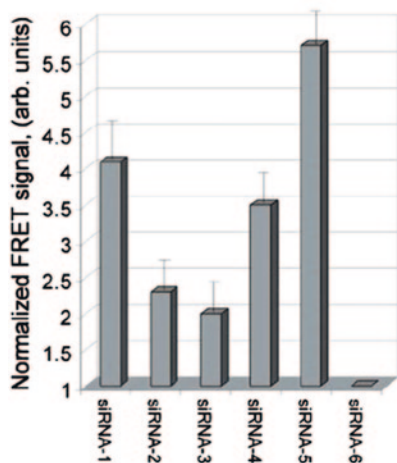
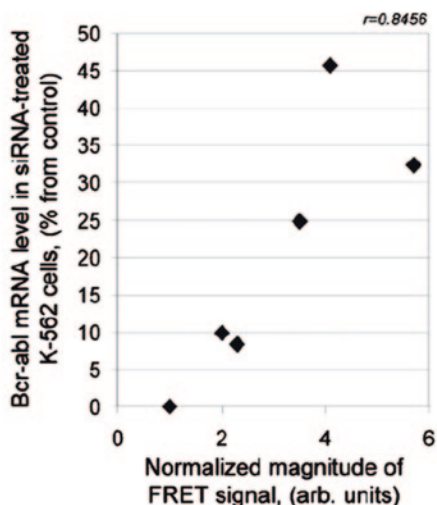
**Fig. 3.10** Schematics of QD-nanobarcode microbead system for high-throughput gene expression analysis. **a** Pseudocolor picture of the microbeads embedded with QDs. **b** Example spectra of the beads coded with different mixture of QDs. **c** Construction of the nanobarcode microbeads. Each bead has a distinctive ratio of four different QDs, allowing identification by a characteristic spectral nanobarcode. The transcript-specific oligonucleotide probes are conjugated with the bead surface. Therefore, each spectral-barcode bead detects a specific oligonucleotide determined by the probe. **d** Gene expression monitoring and quantification sandwich assay. The nanobarcode microbead-attached oligo probes capture biotinylated cRNA sample through hybridization, the cRNA is further sandwiched by the 655-nm streptavidin QDs (or 705, 800 nm) to be quantified. The gene expression variation is measured by fluorescence levels upon imaging with the Mosaic scanner (Quantum Dot Corp.). Reproduced with permission from Ref. [35]. Copyright 2006, American Chemical Society

and coated onto the microbeads to generate a nanobarcode microbead termed as QBeads. Gene-specific oligonucleotide probes are conjugated with the surface of each spectrally nanobarcode bead to create a multiplexed panel, and biotinylated cRNAs are generated from sample total RNA and hybridized to the gene probes on the microbeads. A fifth streptavidin Qdot (655 nm or infrared Qdot) binds to biotin on the cRNA, acting as a quantification reporter. Target identity was decoded based on spectral profile and intensity ratios of the four coding Qdots (525, 545, 565, and 585 nm). The intensity of the 655 nm Qdot reflects the level of biotinylated cRNA captured on the beads and provides the quantification for the corresponding target gene. It provides increased flexibility, convenience, and cost-effectiveness in comparison with conventional gene expression profiling methods.

### 3.2.2 *Foster (or Fluorescence) Resonance Energy Transfer System*

Several studies have demonstrated the effective use of QD FRET donors to detect small analytes by utilizing a common strategy that relies on conjugating QDs with target-binding receptors, which can be either proteins [36, 37], antibody fragments [38, 39], or DNA aptamers [40, 41]. FRET and QDs were also employed for RNA analysis. For example, a single-stranded siRNA conjugated with QD was designed and used as a hybridization probe for the development of a comparatively simple and rapid procedure for preliminary screening of highly effective siRNA sequences for RNA interference (RNAi) in mammalian cells (Fig. 3.11) [42]. The target mRNA was amplified in the presence of Cy5-labeled nucleotides, and Cy5-labeled mRNA served as a hybridization sample. The accessibility and affinity of the siRNA sequence for the target mRNA site were determined by FRET between a QD (donor) and a fluorescent dye molecule (Cy5, acceptor) localized at an appropriate distance from each other when hybridization occurred. The FRET signal was observed only when there was high accessibility between an antisense siRNA and a sense mRNA and did not appear in the case of mismatch siRNAs. This method can markedly facilitate the screening of truly effective siRNAs and significantly shorten the time-consuming siRNA screening procedures.

To improve the detection sensitivity, flexibility, and adaptability, various new strategies have been developed, such as rolling circle amplification [43], isothermal amplification [44], and isothermal strand-displacement polymerase reaction [45]. A novel miRNA detection method based on the two-stage exponential amplification reaction (EXPAR) and a single QD-based nanosensor was developed (Fig. 3.12) [46]. EXPAR provides high amplification efficiency, which can rapidly amplify short oligonucleotides ( $10^6$ – $10^9$ -fold) within minutes. The two-stage EXPAR involved two templates and two-stage amplification reactions under isothermal conditions [47]. The first-stage reaction (Fig. 3.12a, b) was an exponential amplification with the involvement of the  $X'$ – $X'$  template, which enabled the amplification of miRNA. The second-stage reaction (Fig. 3.12c) was a linear amplification with the

**(a) Principle of detection of FRET-efficiency between QD-labeled siRNA and Cy5-labeled target mRNA.****(b) FRET between QD-labeled siRNAs and Cy5-labeled target mRNA****(c) Correlation between FRET signal and RNAi efficiency of anti-bcr-abl siRNAs**

**Fig. 3.11** Efficiency of interaction between siRNA hybridization probes and bcr/abl mRNA hybridization samples-FRET analysis. **a** Typical fluorescent spectra of nonhybridized and hybridized QD-labeled siRNA probe and Cy5-labeled mRNA sample (lex) 420 nm. 1: QD-siRNA-6 (mismatch). 2: QD-siRNA-6 plus Cy5-labeled mRNA. 3: QD-siRNA-5 plus Cy5-labeled mRNA. **b** FRET between QD-labeled siRNAs and Cy5-labeled target mRNA. The results on histograms represent the mean (SD from seven-independent experiments for siRNA-1, 2, and 6, and from six independent experiments for siRNA-3, 4, and 5. **c** Correlation between FRET data (obtained in this study) and effect of anti-bcr/abl siRNAs on the level of target mRNA (obtained from the literature),  $r$  is the correlation coefficient. Reproduced with permission from Ref. [42]. Copyright 2005, American Chemical Society



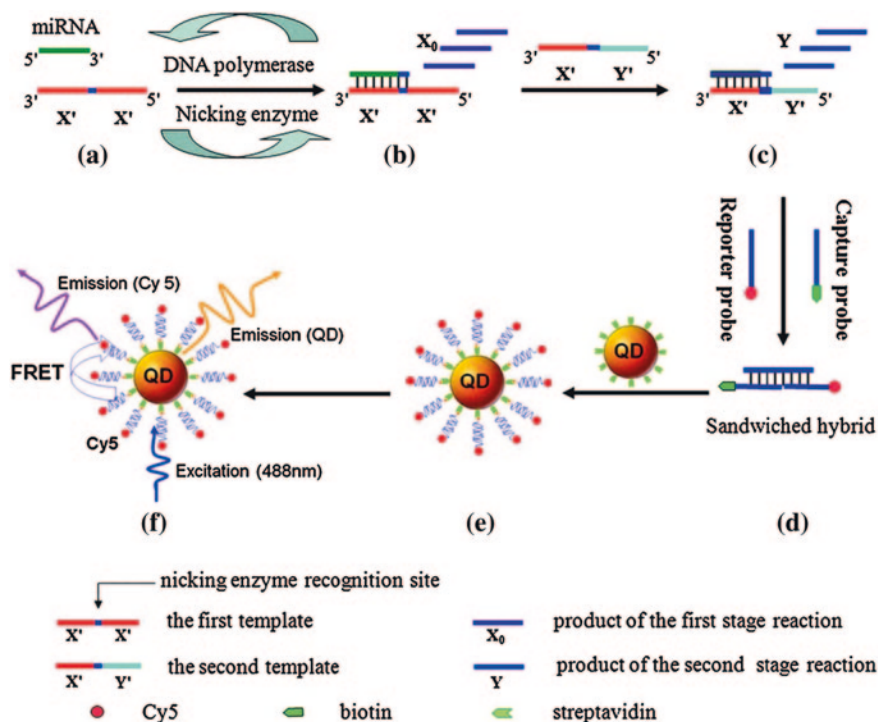


**Fig. 3.12** Scheme of the miRNA assay based on the two-stage EXPAR and single QD-based nanosensor. Reproduced with permission from Ref. [46]. Copyright 2012, American Chemical Society

involvement of the X'-Y' template, which enabled the conversion of miRNA to the reporter oligonucleotide Y. The newly formed reporter oligonucleotide Y cannot in turn prime the X'-Y' template, thus resulting in a linear amplification (Fig. 3.12c). After amplification, the reporter oligonucleotide Y was sandwiched by a biotinylated capture probe and a Cy5-labeled reporter probe (Fig. 3.12d). This sandwich hybrid was then assembled on the surface of a 605QD to form the 605QD/reporter oligonucleotide Y/Cy5 complex through specific biotin-streptavidin binding (Fig. 3.12e). When this complex was excited by a 488-nm argon laser, the fluorescence signals of 605QD and Cy5 were observed simultaneously due to FRET from 605QD to Cy5 (Fig. 3.12f). Isothermal amplification and the single QD-based nanosensor offer improved sensitivity and selectivity for miRNA assay.

### 3.2.3 Sensing Based on DNA-Scaffolded Metal Nanoclusters

Recently, the emergence of noble metal nanoclusters as a novel type of robust and promising fluorescence materials offers great potential for biological labeling, bio-sensing, bioimaging, and diagnostic applications [48–50]. They typically consist

of a few atoms and possess molecular-like optical properties, which are complementary to those of organic dyes and QDs. Particularly, oligonucleotide-templated nanoclusters have drawn increasing attention as a fascinating class of fluorophores due to their amazing features of facile synthesis, ultrafine size, and outstanding spectral and photophysical properties. Using the fluorescence properties of DNA–nanosilver clusters (DNA–AgNC), a DNA–AgNC probe that can detect the presence of target miRNA has been designed (Fig. 3.13) [51]. On the basis of the work of Richards et al., a sequence was chosen as scaffold to successfully create a red-emitting AgNC (DNA-12nt-RED: 5'-CCTCCTTCCTCC-3') [52]. DNA-12nt-RED created red-emissive AgNCs, with an emission maximum at 620 nm, molar extinction coefficient of  $120,000 \text{ M}^{-1}\text{cm}^{-1}$ , fluorescence decay time of 2.23 ns, and a fluorescence quantum yield of 32 %. Therefore, the DNA-12nt-RED would be an ideal candidate to be used for developing a DNA-based probe for miRNA detection. In order to create the probe for detecting miRNA, the complementary DNA sequence of RNA-miR160 was attached to the DNA-12nt-RED sequence. Just like DNA-12nt-RED, after addition of  $\text{AgNO}_3$  and reduction with  $\text{NaBH}_4$ , the DNA-12nt-RED-160 probe displayed strong red emission from the AgNCs. Moreover, the speed of AgNC formation is faster and the overall fluorescence intensity is about 100 times higher in the DNA-12nt-RED-160 probe versus DNA-12nt-RED. The reason is likely that DNA-12nt-RED-160 probe could form a self-dimer or a hairpin structure in the absence of miRNA. In the presence of an increasing concentration of RNA-miR160 sequences, the observed red fluorescence decreased, demonstrating that the DNA-12nt-RED-160 probe can be used for detecting the RNA-miR160 target molecules by monitoring the generated red fluorescence of the AgNCs.

A facile detection of microRNA by target-assisted isothermal exponential amplification (TAIEA) coupled with fluorescent DNA-scaffolded AgNC was also investigated (Fig. 3.14) [53]. The TAIEA reaction utilizes a unimolecular DNA containing three functional domains as the amplification template, polymerases, and nicking enzymes as mechanical activators and target miRNA as the trigger, which enables

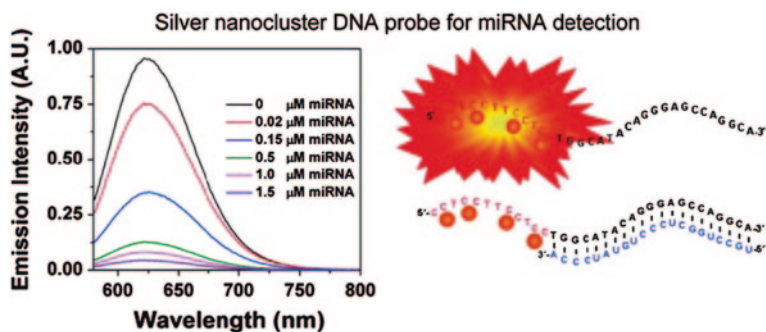


**Fig. 3.13** Scheme of the miRNA assay based on silver nanocluster DNA probe. Reproduced with permission from Ref. [51]. Copyright 2011, American Chemical Society

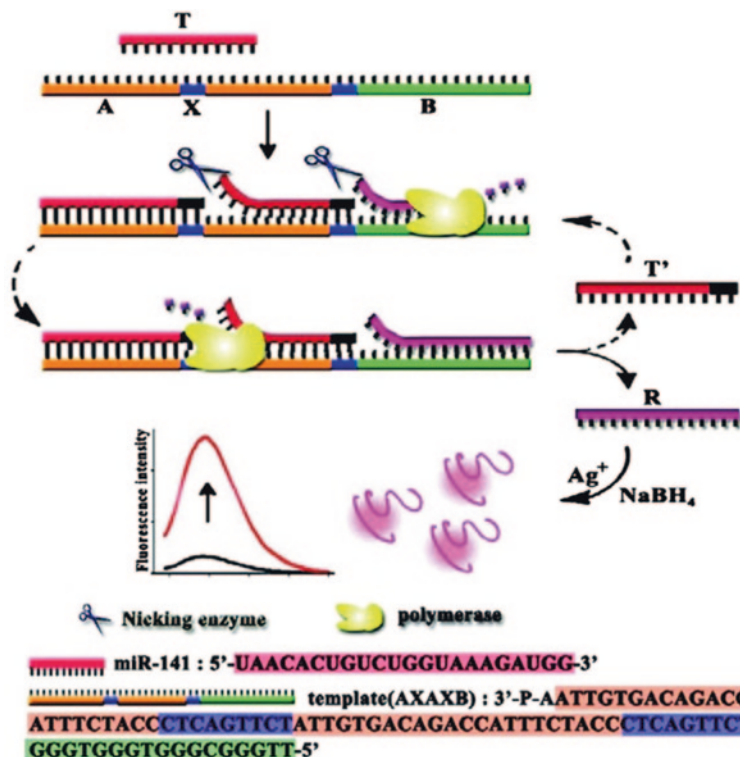
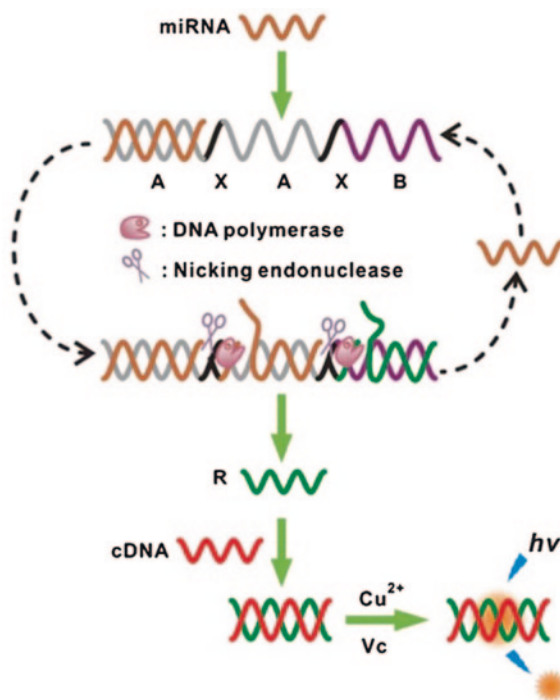


**Fig. 3.14** Detection of miRNA with attomolar sensitivity based on target-assisted isothermal exponential amplification (TAIEA) coupled with fluorescent DNA-templated AgNC probe. Reproduced with permission from Ref. [53]. Copyright 2012, American Chemical Society

the conversion of miRNA to a great amount of the reporter oligonucleotides R within minutes. After amplification, the reporter oligonucleotide R was acting as a scaffold for the synthesis of fluorescent silver nanoclusters in the presence of  $\text{Ag}^+$  through the reduction of  $\text{NaBH}_4$ . The DNA-AgNCs displayed fluorescence emission at 644 nm upon the excitation at 574 nm, functioning as signal indicators in a label-free and environmental-friendly format. The method reveals superior sensitivity with a detection limit of miRNA of 2 aM synthetic spike-in target miRNA under pure conditions (approximately 15 copies of a miRNA molecule in a volume of 10  $\mu\text{L}$ ) and can detect at least a 10 aM spike-in target miRNA in cell lysates.

DNA-AgNCs have attracted an explosion of interest in biological analysis. However, they have one major problem in practical application, that is,  $\text{Ag}^+$  ions can easily form an insoluble product with many general anions, such as  $\text{Cl}^-$  or  $\text{SO}_4^{2-}$ , to terminate the formation of AgNCs. In addition, the DNA-AgNCs formation by the reduction of  $\text{Ag}^+$  ions with  $\text{NaBH}_4$  usually takes one to several hours. In contrast to DNA-AgNCs, the newly emerging CuNCs, selectively formed on a DNA duplex [54–56], offer excellent potential for “on the spot”

**Fig. 3.15** Schematic illustration of miRNA detection using a novel fluorescence probe of dsDNA-templated copper nanoclusters as the signal output, via the target-triggered isothermal exponential amplification reaction. Reproduced with permission from Ref. [57]. Copyright 2013, Royal Society of Chemistry



testing with a rapid and simple “mix-and-measure” format. dsDNA–CuNCs can be readily prepared by reducing  $\text{Cu}^{2+}$  ions with ascorbic acid in the presence of a DNA duplex within fifteen minutes. More importantly, the  $\text{Cu}^{2+}$  ions are soluble in many detection environments and so have no precipitation phenomena like the  $\text{Ag}^+$  ions. Therefore, a facile label-free method for sensitive and selective detection of miRNAs using dsDNA–CuNCs as fluorescent reporters was developed (Fig. 3.15) [57]. In order to improve the analytical sensitivity, they have introduced the target-triggered isothermal exponential amplification reaction (TEIAR) to the proposed method. This amplification strategy has shown great potential as the point-of-care testing with high amplification efficiency under a constant temperature.

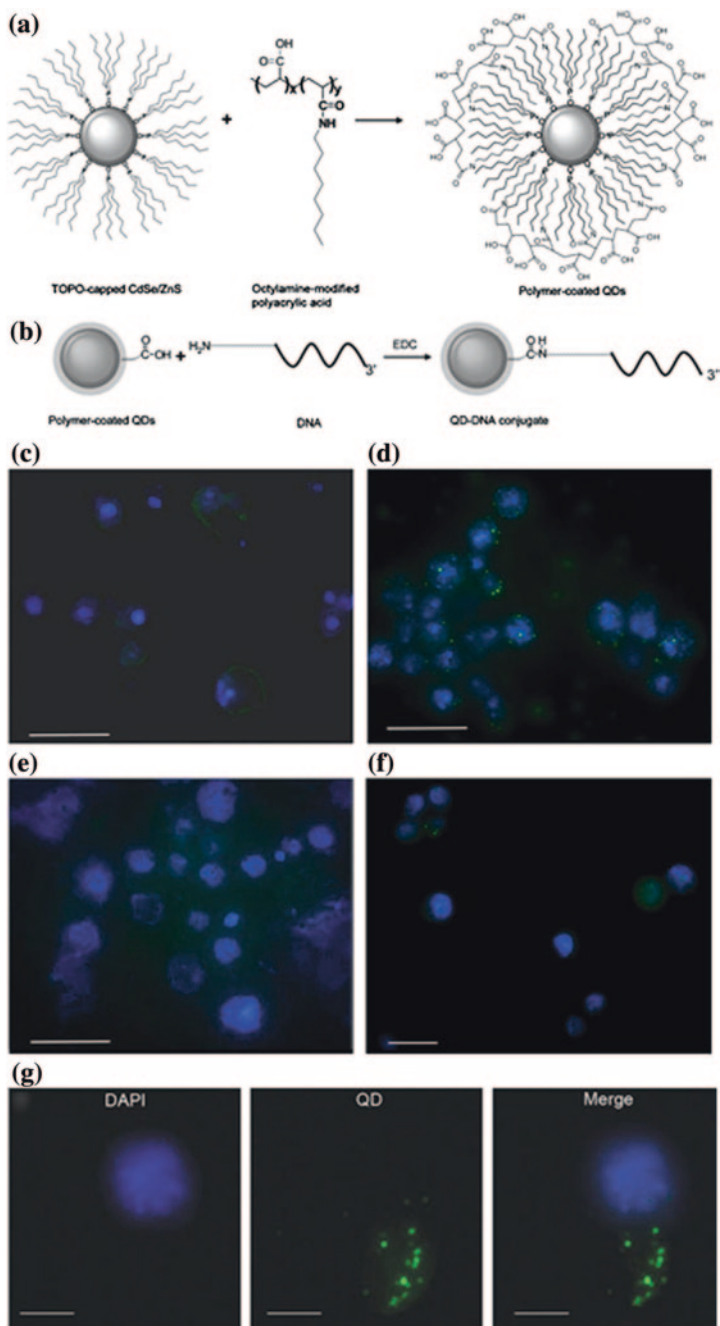
### 3.2.4 Sensing Based on Fluorescence In Situ Hybridization

In situ detection of RNAs is becoming increasingly important for analysis of gene expression within and between intact cells in tissues. Fluorescence in situ hybridization (FISH) of nucleic acid-labeled probes provides a direct visualization of the spatial location of specific DNA or RNA sequences at a particular cellular or chromosomal site and in tissue sections [58]. Streptavidin-labeled/biotinylated

DNA probes have been used for FISH detection of several mRNA targets [59, 60]. However, QDs containing cadmium such as CdSe or CdTe are always toxic due to the release of  $\text{Cd}^{2+}$ . In view of the inherent toxicity of the cadmium, an additional nontoxic ZnS shell was coated onto the CdSeTe/CdS QDs to minimize the toxicity of NIR-emitting QDs [35, 61]. Trioctylphosphine oxide (TOPO)-capped CdSe/ZnS QDs was prepared to reduce cytotoxicity of QDs [62]. Amine-modified oligonucleotide probes are designed and covalently attached to the carboxyl-terminated polymer-coated QDs via EDC chemistry (shown in Fig. 3.16). The resulting QD–DNA conjugates show sequence-specific hybridization with target mRNAs. QD–DNA probes exhibit excellent sensitivity to detect the low-expressing dorsal-related immunity factor gene. Importantly, multiplex FISH of ribosomal protein 49 and actin 5C using green and red QD–DNA conjugates allows the observation of cellular distribution of the two independent genes simultaneously.

### 3.3 QDs for DNA Microarrays

DNA microarrays (also commonly called gene chips, DNA chips, or biochips) are a collection of microscopic DNA spots attached to a solid surface, such as glass, plastic, or silicon supports [63, 64]. They were born for the simultaneous analysis of the expression levels of numerous genes in a single experiment [65]. Since their development in the mid-1990s, DNA microarrays have displayed enormous potentials in various applications, such as cancer diagnosis or drug influence on the gene expression level. DNA microarray technology has revealed a great deal about the genetic factors involved in a number of diseases, including multiple forms of cancer. At the beginning, microarrays were just employed for the identification of the differences in gene expression between normal cells and their cancerous counterparts. Later on, researchers began to apply this technology to distinguish specific subtypes of certain cancers, as well as to determine which treatment methods would most likely be effective for particular patients. This also reflected the effect of medicines which was benefit for drug selection [66, 67]. DNA microarrays are usually categorized as complementary DNA (cDNA) arrays, using either short (25–30 mer) or long ODN (60–70 mer) probes. The core principle behind microarrays lies in their ability to provide a powerful high-throughput system that allows for large-scale analysis of gene expression, genetic alterations, and signal transduction pathways, which can give important information for disease diagnosis, prognostics, and therapeutics. A typical DNA microarray usually consists of the following step: First robotically printing oligonucleotides or cDNA clone inserts onto a glass slide, then one or more fluorescent-labeled cDNA probes generated from samples are hybridized to the surface, later a laser is employed to excite the dye labels and record the fluorescent intensities by a laser confocal fluorescent scanner. Finally, the ratio of fluorescent intensities provides the basis for further meta-analyses. The feasibility



◀ **Fig. 3.16** Scheme for polymer coating of QD–TOPO (a) and the conjugation reaction with amine-terminated oligonucleotides using EDC-coupling reagent (b). Specificity of QD–DNA probes hybridization in situ to detect mRNA (Rp49) in fixed *Drosophila* S2 cells. c Control (QD555 alone, no DNA attached). d QD555–DNA conjugate. e Control experiment with QD555–noncomplementary DNA conjugate. f RNase A treatment 10 mg mL prior to cell fixation significantly decreased the FISH signal. g Representative single-cell FISH image separately displaying a DAPI-stained cell nucleus and the QD–DNA conjugates (for Rp49) exclusively located in the cytoplasm, and the merged image of the DAPI signal and QD555 signal. Reproducibility was obtained from three separate experiments. The scale bar indicates 20 mm (c–f) and 5 mm (g). Reproduced with permission from Ref. [62]. Copyright 2009, Wiley

of QDs in such DNA microarray is ascribed to the narrow multicolor emissions under a single-source excitation. Meissner et al. developed a QD-embedded microsphere-based fluid DNA microarray. CdSe/ZnS QDs embedded in polystyrene microspheres were labeled with DNA oligonucleotides for target capture, and the result was recorded by a high-speed readout flow cytometer [68]. QD-based cDNA microarray was also developed for single-nucleotide polymorphism (SNP) mutation detection in the human p53 tumor suppressor gene and multiallele detections. The authors established a model that used a SNP located at amino acid residue 248, on exon 7 of p53, which is one of the most common mutation hot spots in p53 [69]. As shown in Fig. 3.17, multicolor targeting of SNP mutations in human oncogene p53 and of human hepatitis B and C viruses with different DNA–QDs were realized, which displayed the great potential of DNA–QD conjugates as efficient probes in cDNA microarrays for an ultrafast detection of a great number of viral or bacterial pathogens simultaneously. However, this model system was not extended to real samples such as blood [70].

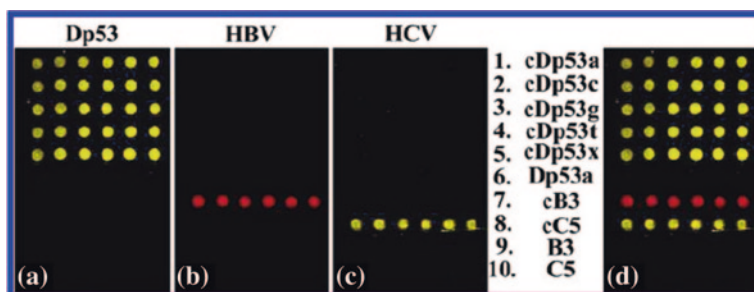


**Fig. 3.17** Multicolor targeting of SNP mutations in human oncogene p53 (rows 1–6) and of human hepatitis B and C viruses (rows 7–10) with different DNA–QD probes. In panel a, yellow Dp53 g-QDs are targeted only toward mutations in human oncogene p53, but SNP detection is not achieved. In panel b, red B3-QDs are targeted toward the hepatitis B virus sequence. In panel c, yellow C5-QDs are targeted only toward the hepatitis C virus sequence. Panel d is an overlay of panels a–c. In both red and yellow channels, signal-to-noise ratio is >100, and no cross talk is observed. Reproduced with permission from Ref. [70]. Copyright 2003, American Chemical Society

## References

1. Lu HC, Schops O, Woggon U, Niemeyer CM (2008) Self-assembled donor comprising quantum dots and fluorescent proteins for long-range fluorescence resonance energy transfer. *J Am Chem Soc* 130(14):4815–4827
2. Sapsford KE, Berti L, Medintz IL (2006) Materials for fluorescence resonance energy transfer analysis: beyond traditional donor-acceptor combinations. *Angew Chem Int Ed Engl* 45(28):4562–4589
3. Tu DT, Liu LQ, Ju Q, Liu YS, Zhu HM, Li RF, Chen XY (2011) Interfacial self-assembly of cell-like filamentous microcapsules. *Angew Chem Int Ed* 50(28):6306–6310
4. Jares-Erijman EA, Jovin TM (2003) FRET imaging. *Nat Biotechnol* 21(11):1387–1395
5. Clapp A, Medintz IL, Fisher BR, Anderson GP, Mattoussi H (2005) Can luminescent quantum dots be efficient energy acceptors with organic dye donors? *J Am Chem Soc* 127:1242–1250
6. Chen GW, Song FL, Xiong XQ, Peng XJ (2013) Fluorescent nanosensors based on fluorescence resonance energy transfer (FRET). *Ind Eng Chem Res* 52(33):11228–11245
7. Noor MO, Krull UJ (2013) Paper-based solid-phase multiplexed nucleic acid hybridization assay with tunable dynamic range using immobilized quantum dots as donors in fluorescence resonance energy transfer. *Anal Chem* 85(15):7502–7511
8. Zhang CL, Xu J, Zhang SM, Ji XH, He ZK (2012) One-pot synthesized DNA-CdTe quantum dots applied in a biosensor for the detection of sequence-specific oligonucleotides. *Chem Eur J* 18:8296–8300
9. Cui DX, Pan BF, Zhang H, Gao F, Wu RN, Wang JP, He R, Asahi T (2008) Self-assembly of quantum dots and carbon nanotubes for ultrasensitive DNA and antigen detection. *Anal Chem* 80:7996–8001
10. Chou CC, Huang YH (2012) Nucleic acid sandwich hybridization assay with quantum dot-induced fluorescence resonance energy transfer for pathogen detection. *Sensors* 12(12):16660–16672
11. Vannoy CH, Chong L, Le C, Krull UJA (2013) Competitive displacement assay with quantum dots as fluorescence resonance energy transfer donors. *Anal Chim Acta* 759:92–99
12. Medintz IL, Berti L, Pons T, Grimes AF, English DS, Alessandrini A, Facci P, Mattoussi H (2007) A reactive peptidic linker for self-assembling hybrid quantum dot-DNA bioconjugates. *Nano Lett* 7(6):1741–1748
13. Yeh H-Y, Yates MV, Mulchandani A, Chen W (2010) Molecular beacon—quantum dot—Au nanoparticle hybrid nanoprobe for visualizing virus replication in living cells. *Chem Commun* 46:3914–3916
14. Kim JH, Chaudhary S, Ozkan M (2007) Multicolor hybrid nanoprobe of molecular beacon conjugated quantum dots: FRET and gel electrophoresis assisted target DNA detection. *Nanotechnology* 18:195105–195112
15. Tan L, Li Y, Drake TJ, Moroz L, Wang K, Li J, Munteanu A, Chaoyong JY, Martinez K, Tas W (2005) Molecular beacons for bioanalytical applications. *Analyst* 130:1002–1005
16. Zhang BQ, Zhang YJ, Mallapragada SK, Clapp AR (2011) Sensing polymer/DNA polyplex dissociation using quantum dot fluorophores. *ACS Nano* 5(1):129–138
17. Wu YZ, Eisele K, Doroshenko M, Algara-Siller G, Kaiser U, Koynov K, Weil T (2012) A quantum dot photoswitch for DNA detection, gene transfection, and live-cell imaging. *Small* 8(22):3465–3475
18. Smith AM, Dave S, Nie SM, True L, Gao XH (2006) Multicolor quantum dots for molecular diagnostics of cancer. *Expert Rev Mol Diagn* 6(2):231–244
19. Han MY, Gao XH, Su JZ, Nie SM (2001) Quantum-dot-tagged microbeads for multiplexed optical coding of biomolecules. *Nat Biotech* 19:631–635
20. Zhang CY, Yeh HC, Kuroki MT, Wang TH (2005) Single-quantum-dot-based DNA nanosensor. *Nature Mater* 4:826–831
21. Zhang CY, Hu J (2010) Single quantum dot-based nanosensor for multiple DNA detection. *Anal Chem* 82:1921–1927



22. Zhou J, Wang QX, Zhang CY (2013) Liposome-quantum dot complexes enable multiplexed detection of attomolar DNAs without target amplification. *J Am Chem Soc* 135:2056–2059
23. Giri S, Sykes EA, Jennings TL, Chan WCW (2011) Rapid screening of genetic biomarkers of infectious agents using quantum dot barcodes. *ACS nano* 5(3):1580–1587
24. Cheng YQ, Zhang X, Li ZP, Jiao XX, Wang YC, Zhang YL (2009) Highly sensitive determination of microRNA using target-primed and branched rolling-circle amplification. *Angew Chem Int Ed* 121:3318–3322
25. Wang H, Ach RA, Curry B (2007) Direct and sensitive miRNA profiling from low-input total RNA. *RNA* 13:151–159
26. Arenz C (2006) MicroRNAs—zukünftige Wirkstoff-Targets? *Angew Chem Int Ed* 118:5170–5172
27. Raymond CK, Roberts BS, Garrett-Engele P, Lim LP, Johnson JM (2005) Simple, quantitative primer-extension PCR assay for direct monitoring of microRNAs and short-interfering RNAs. *RNA* 11:1737–1744
28. Lagos-Quintana M, Rauhut R, Lendeckel W, Tuschl T (2001) Identification of novel genes coding for small expressed RNAs. *Science* 294:853–858
29. Tu YQ, Wu P, Zhang H, Cai CX (2012) Fluorescence quenching of gold nanoparticles integrating with a conformation-switched hairpin oligonucleotide probe for microRNA detection. *Chem Commun* 48:10718–10720
30. Li W, Ruan KC (2009) MicroRNA detection by microarray. *Anal Bioanal Chem* 394:1117–1124
31. Gao ZQ, Peng YF (2011) MicroRNA detection by microarray. *Biosens Bioelectron* 26:3768–3773
32. Cui ZQ, Ren Q, Wei HP, Chen Z, Deng JY, Zhang ZP, Zhang XE (2011) Quantum dot-aptamer nanoprobe for recognizing and labeling influenza A virus particles. *Nanoscale* 3:2454–2457
33. Bi S, Zhou H, Zhang SS (2010) A novel synergistic enhanced chemiluminescence achieved by a multiplex nanoprobe for biological applications combined with dual-amplification of magnetic nanoparticles. *Chem Sci* 1:681–687
34. Liang RQ, Li W, Li Y, Tan CY, Li JX, Jin YX, Ruan KC (2005) An oligonucleotide microarray for microRNA expression analysis based on labeling RNA with quantum dot and nano-gold probe. *Nucleic Acids Res* 33:e17
35. Eastman PS, Ruan WM, Doctolero M, Nuttall R, Feo GD, Park JS, Chu JSF, Cooke P, Gray JW, Li S, Chen FQF (2006) Qdot nanobarcode for multiplexed gene expression analysis. *Nano Lett* 6:1059–1064
36. Li LL, Chen Y, Lu Q, Ji J, Shen YY, Xu M, Fei R, Yang GH, Zhang K, Zhang JR, Zhu JJ (2013) Electrochemiluminescence energy transfer-promoted ultrasensitive immunoassay using near-infrared-emitting CdSeTe/CdS/ZnS quantum dots and gold nanorods. *Scientific Reports* 3:1529
37. Wagh A, Jyoti F, Mallik S, Qian S, Leclerc E, Law B (2013) Polymeric nanoparticles with sequential and multiple FRET cascade mechanisms for multicolor and multiplexed imaging. *Small* 9(12):2129–2139
38. Zhu D, Jiang XX, Zhao CE, Sun XL, Zhang JR, Zhu JJ (2010) Green synthesis and potential application of low-toxic Mn: ZnSe/ZnS core/shell luminescent nanocrystals. *Chem Commun* 46:5226–5228
39. Liang GX, Pan HC, Li Y, Jiang LP, Zhang JR, Zhu JJ (2009) Near infrared sensing based on fluorescence resonance energy transfer between Mn: CdTe quantum dots and Au nanorods. *Biosens Bioelectron* 24(12):3693–3697
40. Sharon E, Freeman R, Willner I (2010) CdSe/ZnS quantum dots-G-quadruplex/hemin hybrids as optical DNA sensors and aptasensors. *Anal Chem* 82:7073–7077
41. Dong HF, Gao WC, Yan F, Ji HX, Ju HX (2010) Fluorescence resonance energy transfer between quantum dots and graphene oxide for sensing biomolecules. *Anal Chem* 82:5511–5517
42. Bakalova R, Zhelev Z, Ohba H, Baba Y (2005) Quantum dot-conjugated hybridization probes for preliminary screening of siRNA sequences. *J Am Chem Soc* 127:11328–11335

43. Bi S, Ji B, Zhang ZP, Zhu JJ (2013) Metal ions triggered ligase activity for rolling circle amplification and its application in molecular logic gate operations. *Chem Sci* 4:1858–1863
44. Li CP, Li ZP, Jia HX, Yan JL (2011) One-step ultrasensitive detection of microRNAs with loop-mediated isothermal amplification (LAMP). *Chem Commun* 47:2595–2597
45. Dong HF, Zhang J, Ju HX, Lu HT, Wang SY, Jin S, Hao KH, Du HW, Zhang XJ (2012) Highly sensitive multiple microRNA detection based on fluorescence quenching of graphene oxide and isothermal strand-displacement polymerase reaction. *Anal Chem* 84(10):4587–4593
46. Zhang Y, Zhang CY (2012) Sensitive detection of microRNA with isothermal amplification and a single-quantum-dot-based nanosensor. *Anal Chem* 84:224–231
47. Tan E, Wong J, Nguyen D, Zhang Y, Erwin B, Van Ness LK, Baker SM, Galas DJ, Niemz A (2005) Isothermal DNA amplification coupled with DNA nanosphere-based colorimetric detection. *Anal Chem* 77:7984–7992
48. Liu CG, Calin GA, Meloon B, Gamliel N, Sevignani C, Ferracin M, Dumitru CD, Shimizu M, Zupo S, Dono M, Alder H, Bullrich F, Negrini M, Croce CM (2004) An oligonucleotide microchip for genome-wide microRNA profiling in human and mouse tissues. *Proc Natl Acad Sci USA* 101:9740–9744
49. Lim LP, Lau NC, Garrett-Engle P, Grimson A, Schelter JM, Castle J, Bartel DP, Linsley PS, Johnson JM (2005) Microarray analysis shows that some microRNAs downregulate large numbers of target mRNAs. *Nature* 433:769–773
50. Zhang M, Guo SM, Li YR, Zuo P, Ye BC (2012) A label-free fluorescent molecular beacon based on DNA-templated silver nanoclusters for detection of adenosine and adenosine deaminase. *Chem Commun* 48:5488–5490
51. Yang SW, Vosch T (2011) Rapid detection of microRNA by a silver nanocluster DNA probe. *Anal Chem* 83:6935–6939
52. Richards CI, Choi S, Hsiang JC, Antoku Y, Vosch T, Bongiorno A, Tzeng YL, Dickson RM (2008) Oligonucleotide-stabilized Ag nanocluster fluorophores. *J Am Chem Soc* 130:5038–5039
53. Liu YQ, Zhang M, Yin BC, Ye BC (2012) Attomolar ultrasensitive microRNA detection by DNA-scaffolded silver-nanocluster probe based on isothermal amplification. *Anal Chem* 84:5165–5169
54. Rotaru A, Dutta S, Jentsch E, Gothelf K, Mokhir A (2010) Selective dsDNA-templated formation of copper nanoparticles in solution. *Angew Chem Int Ed* 49:5665–5667
55. Jia X, Li J, Han L, Ren J, Yang X, Wang E (2012) DNA-hosted copper nanoclusters for fluorescent identification of single nucleotide polymorphisms. *ACS Nano* 6:3311–3317
56. Chen J, Liu J, Fang Z, Zeng L (2011) Random dsDNA-templated formation of copper nanoparticles as novel fluorescence probes for label-free lead ions detection. *Chem Commun* 48:1057–1059
57. Wang XP, Yin BC, Ye BC (2013) A novel fluorescence probe of dsDNA-templated copper nanoclusters for quantitative detection of microRNAs. *RSC Adv* 3:8633–8636
58. Bentolila LA, Weiss S (2006) Single-step multicolor fluorescence in situ hybridization using semiconductor quantum dot-DNA conjugates. *Cell Biochem Biophys* 45:59–70
59. Chan P, Yuen T, Ruf F, Gonzalez-Maeso J, Sealfon SC (2005) Method for multiplex cellular detection of mRNAs using quantum dot fluorescent in situ hybridization. *Nucl Acids Res* 33(18):e161
60. Tholouli E, Hoyland JA, Di Vizio D, O'Connell F, MacDermott SA, Twomey D, Levenson R, Liu YJA, Golub TR, Loda M, Byers R (2006) Imaging of multiple mRNA targets using quantum dot based in situ hybridization and spectral deconvolution in clinical biopsies. *Biochem Biophys Res Commun* 348:628–636
61. Shen YY, Li LL, Lu Q, Ji J, Fei R, Zhang JR, Abdel-Halim ES, Zhu J-J (2012) Microwave-assisted synthesis of highly luminescent CdSeTe@ZnS–SiO<sub>2</sub> quantum dots and their application in the detection of Cu(II). *Chem Commun* 48:2222–2224
62. Choi Y, Kim HP, Hong SM, Ryu JY, Han SJ, Song R (2009) In situ visualization of gene expression using polymer-coated quantum-dot-DNA conjugates. *Small* 5(18):2085–2091
63. Wang J (2000) From DNA biosensors to gene chips. *Nucl Acids Res* 28:3011–3016

64. Hahn S, Mergenthaler S, Zimmermann B, Holzgreve W (2005) Nucleic acid based biosensors: the desires of the user. *Bioelectrochemistry* 67:151–154
65. Albelda SM, Shepard JRE (2000) Functional genomics and expression profiling: be there or be square. *Am J Respir Cell Mol Biol* 23:265–269
66. Hoopes L (2008) Genetic diagnosis: DNA microarrays and cancer. *Nature Education* 1:1
67. Shepard JRE (2006) Polychromatic microarrays: simultaneous multicolor array hybridization of eight samples. *Anal Chem* 78(8):2478–2486
68. Meissner KE, Herz E, Kruzelock RP, Spillman WB (2003) Quantum dot-tagged microspheres for fluid-based DNA microarrays. *Phys Stat Sol (C)* 4:1355–1359
69. Pfeifer GP (2000) p53 mutational spectra and the role of methylated CpG sequence. *Mutat Res* 450:155–166
70. Gerion D, Chen FQ, Kannan B, Fu AH, Parak WJ, Chen DJ, Majumdar A, Alivisatos AP (2003) Room-temperature single-nucleotide polymorphism and multiallele DNA detection using fluorescent nanocrystals and microarrays. *Anal Chem* 75(18):4766–4772